

LETTERS

Primary Processes of the Electronic Excited States of *trans*-Urocanic Acid

Bulang Li, Kerry M. Hanson, and John D. Simon*

Department of Chemistry and Biochemistry, University of California at San Diego, 9500 Gilman Drive, La Jolla, California 92093-0341

Received: August 30, 1996; In Final Form: November 6, 1996[⊗]

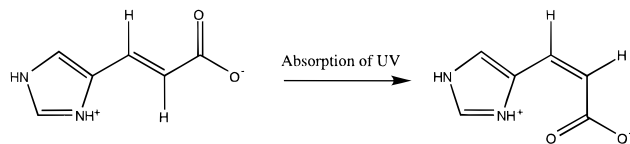
The primary photoreactivity of the excited states of *trans*-urocanic acid (*t*-UA) is investigated by ultrafast transient-absorption spectroscopy. Fundamentally different photophysics were observed when *t*-UA is excited at 266 nm, near the peak of the absorption spectrum, and 306 nm, in the red tail of the absorption spectrum. The data support the conclusion that the wavelength-dependent photophysics of *t*-UA is due to the presence of two different closely spaced electronic states. Excitation at 266 nm populates a $\pi\pi^*$ state that is localized on the imidazole ring. The transient data following photoexcitation of *t*-UA at 266 nm in both a pH 5.6 and a pH 7.2 solution are similar, even though the protonation state of the tertiary nitrogen on the imidazole ring is different at these two pH values. The data therefore support that the photophysics at pH 5.6 and pH 7.2 must involve a common excited state. Steady-state excitation spectra suggest that a proton transfer process from *t*-UA to the solvent occurs following the excitation at 266 nm at pH 5.6, which generates an electronically excited singlet state of the deprotonated molecule. This state is directly accessed by the 266 nm excitation of *t*-UA at pH 7.2. The population in this singlet state decays by intersystem crossing with a rate constant of $1.4 \times 10^{11} \text{ s}^{-1}$. Isomerization is not believed to occur from this triplet state. Excitation of *t*-UA at 306 nm populates an entirely different state, which leads to isomerization. From the observed ground state repopulation dynamics, the minimum rate for the excited state isomerization is $1.2 \times 10^{10} \text{ s}^{-1}$.

1. Introduction

The potential health risks associated with solar UV exposure have become major concerns worldwide because of recent reports of reduced levels of atmospheric ozone¹ and increased incidence of skin cancers.² UV radiation can cause sunburn, photoaging, DNA damage, immunosuppression, and skin cancer. These adverse effects of UV radiation are initiated by the photochemistry of DNA and various other chromophores. For example, one of the major causes of skin cancer is attributed to photodimerization of thymine in the P53 tumor suppresser gene.³ Recently, another epidermal UV chromophore, urocanic acid (UA) (refs 4–10 and references therein), has been implicated as a mediator for UV-induced immunosuppression, as well.

Urocanic acid is a metabolizing product of histidine and represents about 0.7% of the dry weight of the epidermis where it can absorb both UV-A and UV-B radiation. It is synthesized in the uppermost layer of the skin as its *trans* isomer,⁴ where, upon exposure to UV radiation, *trans*-UA can isomerize to *cis*-UA (Scheme 1). A photostationary state with approximately equal amount of both isomers⁵ can be achieved. Because both *trans*- and *cis*-UA absorb in the same wavelength region as DNA, urocanic acid was initially ascribed to behave as a natural sunscreen, protecting DNA from photodamage. As a result, it has been used as an ingredient in suntan lotions. But in 1983, De Fabo and Noonan⁶ proposed that UA could act as a mediator for UV-induced immunosuppression. Currently, research indicates that the isomerization of *trans*-UA to, and the subsequent

[⊗] Abstract published in *Advance ACS Abstracts*, January 15, 1997.

SCHEME 1: Isomerization of *trans*-Urocanic Acid^a

^a The structure drawn is that present in solution at pH 5.6 (the average pH of human sweat). The pK_a of the tertiary nitrogen on the imidazole ring is 5.8, and therefore this site is deprotonated in a pH 7.2 solution.

accumulation of, *cis*-UA leads to immunosuppression and potentially cutaneous carcinogenesis.⁷ Thus, urocanic acid's use in cosmetic products has been withdrawn since the early nineties.⁸

The photochemistry of *trans*-UA has turned out to be complex. For example, Morrison and co-workers reported that while the absorption of *trans*-UA peaks around 270 nm, the quantum efficiency of the *trans* to *cis* isomerization peaks at 310 nm, in the low-energy tail of the absorption spectrum. Studies show that the quantum yield for isomerization is strongly wavelength dependent, ranging from about 0.05 at 266 nm to 0.5 at 310 nm.⁹ To our knowledge, there are no experimental studies that directly probe the excited state dynamics of urocanic acid. Our current knowledge of UA's photophysics is provided by steady-state absorption and emission studies,¹⁰ quantum yield measurements for isomerization,⁹ and triplet-sensitization experiments.¹¹ In this paper, we examine UA's excited state dynamics using femtosecond and picosecond transient-absorption spectroscopy. Transient-absorption experiments were conducted as a function of excitation and probe wavelength and the pH of the solution. The results support the conclusion that the wavelength-dependent photoreactivity of *trans*-UA near 266 and 310 nm is due to the presence of at least two distinct and weakly coupled electronic transitions.

Experimental Section

Transient-absorption experiments requiring subpicosecond time resolution were carried out with a home-built amplified Ti:sapphire laser system with a time resolution of approximately 200 fs. This output of the laser beam was frequency doubled and then tripled using two BBO crystals to obtain the pump wavelength of 266 nm. The pump pulse energy at 266 nm was 2–5 μJ . The residual of the second harmonic output was focused into a water cell to generate a continuum, and various 10 nm band-pass filters were used to select a probe wavelength until a signal was found (340 nm). For the 266 nm degenerate experiments, a glass slide was used to select approximately 5% of the tripled light for the probe beam. The degenerate 306 nm pump–probe experiments were accomplished using a home-built optical parametric amplifier system operating at 1 kHz¹² with a time resolution of 50 fs. The 306 nm light was produced from frequency doubling the amplified 1200 nm OPA output, which was then frequency doubled to generate approximately 1 μJ 306 nm pump pulses. Approximately 5% of this output was used as the probe source. Experiments requiring delays between 1 and 10 ns were carried out using a home-built Nd:YLF regenerative amplification system that has a time resolution of 10 ps. In addition to generating light at the various harmonics, this laser is used to pump a home-built OPG/OPA systems that provides tunable pulses from 300 nm to above 2 μm . Transients acquired on either laser system were found to be independent of the polarization of the pump and probe beams.

t-UA was obtained from Aldrich and used without further purification. The solutions were buffered using HPLC grade water. A pH of 5.6 was maintained by 0.1 M acetate buffer. A

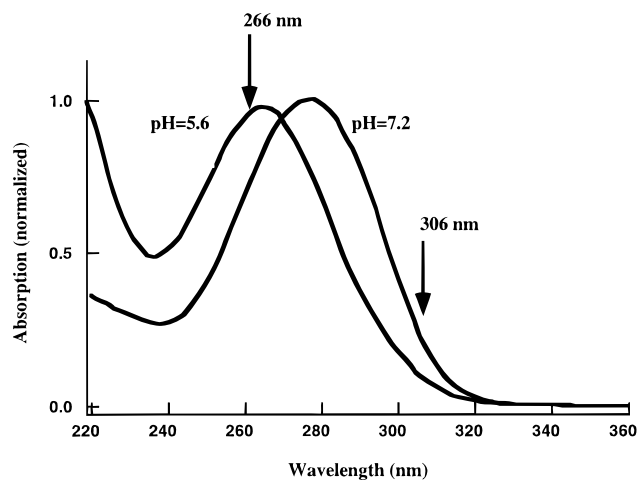


Figure 1. Absorption spectra of *t*-UA in pH 5.6 and 7.2 buffer solution. The excitation wavelengths for transient absorption experiments are marked. The tertiary nitrogen on the imidazole group is protonated at pH 5.6 and deprotonated at pH 7.2.

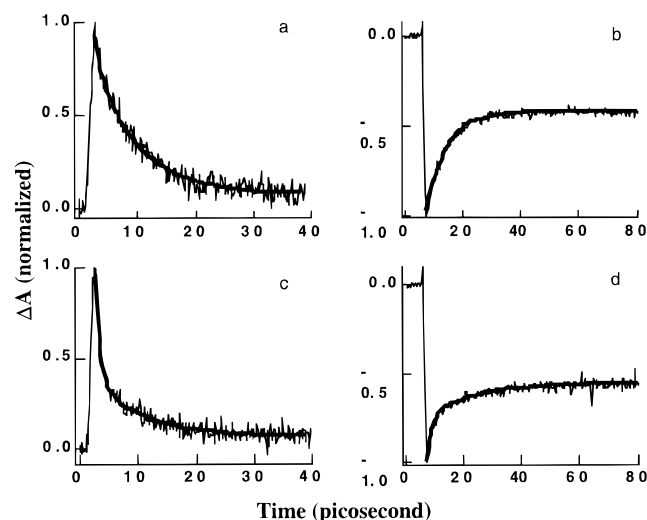


Figure 2. Transient absorption data at 266 nm excitation: (top) in pH 5.6 solution; (bottom) in pH 7.2 solution. Probe wavelength is at 340 nm (a and c) and at 266 nm (b and d).

pH of 7.2 was maintained by 0.1 M potassium phosphate buffer. The concentration of *t*-UA was on the order of 70 μM , and the solutions were flowed through a 1 mm quartz flow cell in order to prevent artifactual signals that could arise from the photo-degradation of the sample. The sample was changed after every data accumulation. A typical run required 20 min, and in this time period, only a negligible amount of *t*-UA is converted to other photochemical products.

Results

Figure 1 shows the absorption spectra of *t*-UA in pH 5.6 and pH 7.2 solutions. The excitation wavelengths used in this study are indicated in the figure. Figure 2a–d presents time-resolved bleaching and absorption data for *t*-UA in both pH 5.6 (2a,b) and pH 7.2 (2c,d) buffer solutions. The excitation wavelength for all four data plots is 266 nm. This wavelength is near the absorption maximum of *t*-UA in the pH 5.6 solution and is on the blue side of the absorption maximum ($\lambda_{\text{max}} = 280 \text{ nm}$) of *t*-UA in the pH 7.2 solution (Figure 1). The probe wavelengths are 266 nm (2b,d) and 340 nm (2a,c). The data observed for the two different pHs are similar. A longer time study (data not shown) of the pump–probe experiment at 266 nm indicates no change in the transient signal up to a delay of 8 ns, the longest

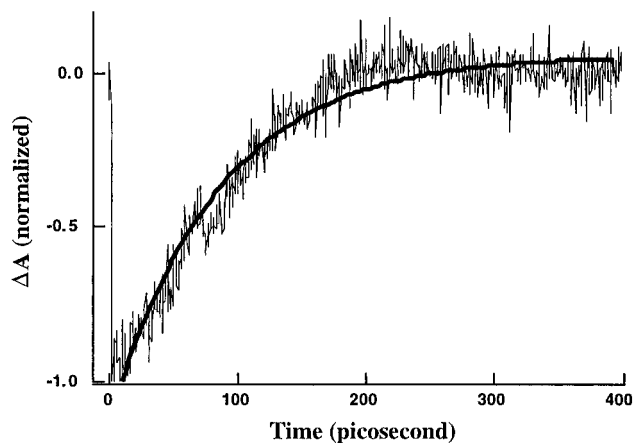


Figure 3. Transient absorption data of *t*-UA in pH 5.6 solution observed for the degenerate 306 nm pump/probe experiment.

delay time studied. Figure 3 shows the transient dynamics observed for a degenerate 306 nm pump–probe experiment of *t*-UA at pH 7.2. In this case, the initial bleach of the absorption shows a complete recovery on the picosecond time scale.

Discussion

As stated above, the isomerization quantum yield of *t*-UA is wavelength dependent. In addition, the emission spectra are wavelength dependent,¹⁰ and the photoacoustic calorimetry signals also depend on the excitation wavelength.¹³ We consider two possible explanations for this wavelength-dependent photoreactivity. First, the broad and structureless UV spectrum could be due to the presence of multiple ground state rotamers that have different absorption spectra and different excited state reactivities. Such a model has been used to describe the wavelength-dependent behavior of bilirubin,¹⁴ diphenylbutadiene,¹⁵ and dihexatriene.¹⁶ Second, the absorption spectrum of *t*-UA could reflect the superposition of two separate absorption transitions. The two excited states accessed would then have different reactivities, and the photophysics from the higher energy state would occur on a time scale short compared to internal conversion. Such a model has been used to describe the behavior of cinnamic acid.¹⁷ This molecule is similar in structure to urocanic acid, with the imidazole replaced by a benzyl group, and has two electronic transitions: a $\pi\pi^*$ dominating the absorption spectrum near the maximum at 280 nm and a weak $n\pi^*$ transition near the red tail of the absorption profile (>300 nm). The transient absorption data suggest that urocanic acid's photochemistry can be described by a model that is similar to that used to describe the wavelength-dependent behavior of cinnamic acid, namely, that the UV absorption band is comprised of overlapping and weakly coupled electronic transitions.

For the photoexcitation of *t*-UA at 266 nm, similar transient absorption dynamics are observed for both pH 5.6 and 7.2 solutions (Figure 2), suggesting that a common excited state of *t*-UA is generated in both solutions. Note though that the ground state configurations do differ at these two pH values. At pH 5.6 the tertiary nitrogen on the imidazole ring is protonated, and at pH 7.2 this site is deprotonated. We propose that at pH 5.6 *t*-UA undergoes rapid (<200 fs) deprotonation in the excited state to generate an electronically excited molecule, which is similar to that created by the direct excitation of *t*-UA at pH 7.2. This proposed reaction is supported by the fluorescence excitation study reported by Shukla and Mishra¹⁰ and confirmed by our laboratory. In these studies, the excitation maximum is found to be independent of the pH (pH 3.2–11) of the solution,

whereas the absorption maximum is highly dependent upon pH—at pH 5.6 the absorption maximum peaks at 266 nm, and at pH 7.2 the absorption peaks at 280 nm (Figure 1). The excitation spectrum for either solution, however, peaks at 280 nm. Therefore, we can conclude that the excited state reached upon excitation at 266 nm is deprotonated on the tertiary nitrogen regardless of pH. Furthermore, the isomerization study reported by Morrison and co-workers shows little pH dependence,⁹ further supporting the generation of a common excited state at the two pH values. The common excited state reached upon excitation at 266 nm for pH 5.6 and pH 7.2 must result from a change in the excited state pK_a of the tertiary nitrogen on the imidazole. The absorption transition must then decrease the electron density on the imidazole ring, making the nitrogen more acidic. Similar phenomena have been observed in a variety of compounds such as aryl alcohols, which show significant decrease of pK_a in their excited electronic state compared to the ground state. For example, 2-naphthol¹⁸ is a weak acid in the ground state ($pK_a = 9.46$) but is a much stronger acid upon excitation to its lowest excited singlet state ($pK_a^* = 2.80$). These observations along with UA's strong oscillator strength near 266 nm (10^4) supports the conclusion that this transition arises most likely from a $\pi \rightarrow \pi^*$ transition within the imidazole ring at either pH.

The data shown in Figure 2 are therefore consistent with the following argument. The dominant contribution to the dynamics observed at the probe wavelength of 340 is the $S_x \rightarrow S_N$ absorption of *t*-UA (with the nitrogen of the imidazole ring deprotonated). (We use S_x instead of S_1 to describe the lower energy state of this transient because excitation at 306 nm at both pH 5.6 and pH 7.2 accesses a lower energy state, which is likely to be a singlet. The dynamics then show that intersystem crossing occurs more rapidly than internal conversion meaning that these two low-energy excited states are weakly coupled.)

The decay in the transient signal reflects the subsequent intersystem crossing process, which can be fit to a first-order kinetic process with a rate constant of $1.4 \times 10^{11} \text{ s}^{-1}$. For a probe wavelength of 266 nm, an initial bleaching of the ground state population is observed, followed by a recovery of the signal to about half of its negative-time value. The recovery dynamics observed in the degenerate 266 nm experiment could, in principle, arise from either the repopulation of the ground state or the population of a long-lived transient absorbing at the same wavelength as the pump wavelength. A triplet state has been shown to exist by Morrison's triplet sensitization¹¹ studies, and the lowest-energy triplet state is estimated to lie approximately 250 kJ/mol above the ground state. We have confirmed this value by photoacoustic experiments.¹³ The time scale of the rise at 266 nm is the same as that of the decay of the data obtained at 340 nm. Such evidence when combined supports the argument that the short-lived transient at 340 nm and the long-lived transient absorbing at 266 nm result from rapid intersystem crossing to a long-lived electronically excited triplet state with $T_x \rightarrow T_n$ absorption at 266 nm.

The 266 nm pump/340 nm probe transient absorption data are slightly different at the two pH values studied. Both contain a 7 ps component, and yet we observe an initial fast decay component (~ 1 ps) at pH 7.2 which is absent at pH 5.6. We tentatively assign the fast component observed at pH 7.2 to a vibrational relaxation process. At pH 7.2, the electronic excited state of *t*-UA lies lower in energy than it does at pH 5.6. This is evidenced by the absorption spectrum of *t*-UA, which red shifts when the pH of the solution is raised (see Figure 1). Therefore, excitation at 266 nm generates a molecule with more excess energy at pH 7.2 than at pH 5.6. As a result, pronounced

vibrational relaxation dynamics appear. At pH 5.6, 266 nm excitation still produces a vibrationally hot (but to a lesser degree) molecule. However, the ultrafast deprotonation reaction that occurs at this pH provides the molecule with an addition channel by which it can dissipate the excess vibrational energy.

Figure 3 displays the transient absorption data for a degenerate pump-probe experiment at 306 nm. Following a bleach at $t = 0$, a full recovery of the signal is observed. The recovery dynamics can be described by a first-order kinetic process with a rate constant of $1.2 \times 10^{10} \text{ s}^{-1}$, which is approximately 10 times greater than the intersystem-crossing rate constant found when pumping at 266 nm and probing at 340 or 266 nm. The dramatic difference in the two rate constants resulting from the two different pump wavelengths is indicative of the wavelength-dependent photoreactivity exhibited by urocanic acid (recall that the isomerization of *trans*- to *cis*-UA is dependent upon excitation wavelength). Morrison determined an isomerization quantum yield of nearly 0.5 at 310 nm but only 0.05 near 266 nm.⁹ It is reasonable then to ascribe the dynamics at 306 nm to be unique from those found at 266 nm, and therefore we attribute the dynamics at 306 nm to result from ground state repopulation, with no intersystem crossing occurring upon excitation of *t*-UA at this wavelength. Because *cis*- and *trans*-UA absorb similarly at 306 nm, the dynamics cannot be used to determine whether or not isomerization occurs. The isomerization quantum yield of 0.5 at approximately 306 nm places a lower limit on the excited state isomerization rate constant of $1.2 \times 10^{10} \text{ s}^{-1}$. Further study is required in order to directly monitor the excited state isomerization process and assess whether or not there is an energy barrier to isomerization along the excited state isomerization reaction coordinate. We are currently constructing a tunable UV source that is to be pumped by our femtosecond Ti-sapphire system, and such studies will be reported at a later date.

Acknowledgment. We thank Chris Bardeen and Vladislav Yakovlev for their help with the 306 nm experiments in the laboratory of Professor Kent Wilson. We thank Peijun Cong for technical assistance. This work is supported by the National Institutes of Health.

References and Notes

- (1) Kerr, J. B.; McElroy, C. T. *Science* **1993**, *262*, 1032.
- (2) Ko, C. B.; Walton, S.; Keczkcs, K.; Bury, H. P. R.; Nicholson, C. *Br. J. Dermatol.* **1994**, *130*, 269.
- (3) Ziegler, A.; Jonason, S.; Leffell, D. M.; Simon, J. A.; Sharma, H. W.; Kimmelman, J.; Remington, L.; Jacks, T.; Brash, D. E. *Nature* **1994**, *372*, 773.
- (4) Scott, I. R. *Biochem. J.* **194**, 829.
- (5) Gibbs, N. K.; Norval, M.; Traynor, N. J.; Wolf, M.; Johnson, B. E.; Crosby, J. *Photochem. Photobiol.* **1993**, *57*, 584.
- (6) De Fabo, E. C.; Noonan, F. P. *J. Exp. Med.* **1983**, *157*, 84–98.
- (7) Matheson, M. J.; Reeve, V. E. *Photochem. Photobiol.* **1991**, *53*, 639.
- (8) Review by the Cosmetic Ingredient Expert Panel. *J. Am. Coll. Toxicol.* **1995**, *14*, 386.
- (9) Morrison, H.; Bernasconi, C.; Pandey, G. *Photochem. Photobiol.* **1984**, *40*, 549.
- (10) Shukla, M. K.; Mishra, P. C. *Spectrochim. Acta* **1995**, *51A*, 831.
- (11) Morrison, H.; Bernasconi, A. C.; Fagan, G. *Photochem. Photobiol.* **1980**, *32*, 711.
- (12) Yakovlev, V. V.; Kohler, B.; Wilson, K. R. *Opt. Lett.* **1994**, *19*, 2000.
- (13) Hanson, K. M.; Li, B.; Simon, J. D. *J. Am. Chem. Soc.*, in press.
- (14) Braslavsky, S. E.; Holzwarth, A. R.; Schaffner, K. *Angew. Chem., Int. Ed. Engl.* **1983**, *22*, 656.
- (15) Wallace-Williams, S. E.; Moller, S.; Goldbeck, R. A.; Hanson, K. M.; Lewis, J. W.; Yee, W. A.; Kligler, D. S. *J. Phys. Chem.* **1993**, *97*, 9587.
- (16) Saltiel, J.; Sears, D. F.; Sun, Y.-P.; Choi, J.-O. *J. Am. Chem. Soc.* **1992**, *114*, 3607.
- (17) Ullman, E. F.; Babad, E.; Singh, P. *J. Am. Chem. Soc.* **1969**, *91*, 5792.
- (18) Lawrence, M.; Marzocco, C. J.; Morton, C.; Schwab, C.; Halpern, A. M. *J. Phys. Chem.* **1991**, *95*, 10294.